An Adult Passive Transfer Mouse Model to Study Desmoglein 3 Signaling in Pemphigus Vulgaris

Katja Schulze[1,2], Arnaud Galichet[1,2], Beyza S. Sayar[1,2], Anthea Scothern[3], Denise Howald[1,2], Hillard Zymann[1], Myriam Siffert[1,2], Denise Zenhäusern[3], Reinhard Bolli[3], Peter J. Koch[4], David Garrod[5,6], Maja M. Suter[1,2] and Eliane J. Müller[1,2]

Evidence has accumulated that changes in intracellular signaling downstream of desmoglein 3 (Dsg3) may have a significant role in epithelial blistering in the autoimmune disease pemphigus vulgaris (PV). Currently, most studies on PV involve passive transfer of pathogenic antibodies into neonatal mice that have not finalized epidermal morphogenesis, and do not permit analysis of mature hair follicles (HFs) and stem cell niches. To investigate Dsg3 antibody-induced signaling in the adult epidermis at defined stages of the HF cycle, we developed a model with passive transfer of AK23 (a mouse monoclonal pathogenic anti-Dsg3 antibody) into adult 8-week-old C57Bl/6J mice. Validated using histopathological and molecular methods, we found that this model faithfully recapitulates major features described in PV patients and PV models. Two hours after AK23 transfer, we observed widening of intercellular spaces between desmosomes and EGFR activation, followed by increased Myc expression and epidermal hyperproliferation, desmosomal Dsg3 depletion, and predominant blistering in HFs and oral mucosa. These data confirm that the adult passive transfer mouse model is ideally suited for detailed studies of Dsg3 antibody-mediated signaling in adult skin, providing the basis for investigations on novel keratinocyte-specific therapeutic strategies.

INTRODUCTION

Pemphigus vulgaris (PV) is a severe autoimmune blistering disease characterized by suprabasal blisters in skin and mucous membranes (Stanley and Amagai, 2006). On average, 90% of PV patients exhibit autoantibodies against desmoglein 3 (Dsg3; Ishii et al., 1997; Amagai et al., 1999a), an intercellular adhesion molecule and component of desmosomes (Garrod et al., 2002). Although the pathogenic mechanism leading to blister formation is not well understood, intracellular signaling has been found to be both involved and necessary in this process. A new paradigm was

[1]Department of Molecular Dermatology, Institute of Animal Pathology, Vetsuisse Faculty, University of Bern, Bern, Switzerland; [2]DermFocus, Vetsuisse Faculty, University of Bern, Bern, Switzerland; [3]CSL Behring AG, Bern, Switzerland; [4]Departments of Dermatology and Cell and Developmental Biology, Charles C Gates Center for Regenerative Medicine and Stem Cell Biology, University of Colorado, Aurora, Colorado, USA; [5]Department of Developmental Biology, Faculty of Life Sciences, University of Manchester, Manchester, UK and [6]King Saud University, Riyadh, Saudi Arabia

Correspondence: Eliane J. Müller, Department of Molecular Dermatology, Institute of Animal Pathology, Vetsuisse Faculty, University of Bern, Länggass-Strasse 122, Postfach 8466, Bern CH-3001, Switzerland. E-mail: eliane.mueller@vetsuisse.unibe.ch

Abbreviations: AK23, mouse monoclonal pathogenic anti-Dsg3 antibody; Dsc3, desmocollin 3; Dsg3, desmoglein 3; HF, hair follicle; mIgG, mouse IgG; PBS, phosphate-buffered saline; PF, pemphigus foliaceus; PG, plakoglobin; PV, pemphigus vulgaris

Received 23 November 2010; revised 5 July 2011; accepted 28 July 2011; published online 29 September 2011

therefore brought forward that Dsg3 and other possible molecular targets in PV govern outside–in signaling (Müller et al., 2008; Getsios et al., 2010).

Over a decade ago, Kitajima and collaborators reported on PV IgG-induced signaling events such as the rapid activation of protein kinase C and phospholipase C (Esaki et al., 1995; Osada et al., 1997). More recently, lack of responsiveness to PV IgG in keratinocytes deleted for the adhesion and signaling molecule plakoglobin (PG) underscored the necessity of a signaling response in PV (Caldelari et al., 2001; de Bruin et al., 2007). To date, passive transfer of PV IgG into neonatal mice, in combination with chemical inhibitors, has confirmed a number of signaling effectors contributing to PV pathophysiology, including EGFR, Myc, p38, phospholipase C/protein kinase C, and Src (Sanchez-Carpintero et al., 2004; Berkowitz et al., 2006; Williamson et al., 2006; Chernyavsky et al., 2007; Pretel et al., 2009). These observations suggest that inhibition of specific signaling molecules represents a potent therapeutic strategy in PV (Getsios et al., 2010).

Myc expression is critical for normal skin homeostasis, in which overexpression in combination with stem cell depletion can lead to epidermal hyperproliferation, hair loss, and spontaneous wounds (Watt et al., 2008). Human PV patients exhibit increased Myc expression and hyperproliferation in epidermis and hair follicles (HFs; Williamson et al., 2006), the sites of Dsg3 expression in human skin (Hanakawa et al., 2004). Moreover, they suffer from increased hair loss (Koch et al., 1998; personal communication

Dr Michael Hertl, University of Marburg, Marburg, Germany). Hair loss due to blisters in the resting (telogen) HF are predominant features of Rag2−/− mice after adoptive transfer of Dsg3−/− splenocytes or AK23 hybridoma cells (producing a pathogenic Dsg3-specific mouse antibody), as well as of *Dsg3*-null mice (Koch *et al.*, 1998; Amagai *et al.*, 2000; Tsunoda *et al.*, 2003). Because of these striking observations, it is of interest to address the consequences of disrupted Dsg3 function in HFs and epidermal stem cell niches in PV.

Currently, neonatal mice are the model system to test PV antibody pathogenicity *in vivo* (Anhalt *et al.*, 1982). However, the morphogenesis of murine epidermis and its appendages including HFs is not finalized until postnatal day 15 (Schneider *et al.*, 2009). Furthermore, after adoptive transfer, adult Rag2−/− mice typically develop blisters over a prolonged incubation time, precluding defined time-course studies on antibody-triggered primary signaling events (Amagai *et al.*, 2000; Tsunoda *et al.*, 2003). Hence, the goal of this study was to establish a mouse model for prospective studies on Dsg3-antibody-initiated signaling in adult skin at defined stages of the HF cycle.

Here we validate the passive transfer of the pathogenic monospecific Dsg3 antibody AK23 into 8-week-old C57Bl/6J mice (which are in the prolonged synchronized telogen HF stage) by focusing on major ultrastructural, biochemical, and signaling parameters observed in PV patients, neonatal mice, human tissue models, and cultured keratinocytes. Our data reveal that this adult mouse model recapitulates major findings in PV, and demonstrate that passive transfer into adult mice represents an ideal tool both to study Dsg3 signaling in adult skin, including HFs and stem cell niches, and to test novel therapeutic strategies in PV.

RESULTS
AK23- and AK23/PF-induced changes in neonatal mice
To validate the response of AK23-injected adult mice against the neonatal model, we first tested whether neonatal mice treated with AK23 recapitulate previous findings obtained with PV IgG (containing Dsg1 antibodies), such as EGFR, p38, and c-Myc activation (Berkowitz *et al.*, 2006; Williamson *et al.*, 2006; Pretel *et al.*, 2009). AK23 was injected alone, and as a control, with a half-pathogenic dose of pemphigus foliaceus (PF) patients' IgG (containing Dsg1 antibodies; AK23/PF; Mahoney *et al.*, 1999).

In agreement with our former results (Williamson *et al.*, 2006), only AK23/PF-injected neonatal mice exhibited epidermal lesions after 24 hours, whereas AK23/PF- and AK23-treated animals showed PV-like lesions in the lip and the hard palate (data not shown). Independently of PF IgG, proliferation was increased in epidermis of all AK23-treated mice as quantified on non-lesional skin sections labeled for the proliferation marker Ki67 (Figure 1a). Back skin protein extracts further revealed significant EGFR activation in AK23/PF- and AK23-treated mice (Figure 1b and c). Phosphorylation sites previously addressed in PV were investigated (Heupel *et al.*, 2009; Pretel *et al.*, 2009). In AK23/PF-treated animals, we observed increased phosphorylation of Tyr845, a Src kinase

substrate, and its phosphorylation was reported to result in receptor activation and mitogenesis in fibroblasts and human breast cancer cells (Ishizawar and Parsons, 2004; Figure 1b). Phosphorylation of Tyr992 and, to a minor extent, Tyr1173 was also increased. P-Tyr992 is a high-affinity binding site for phospholipase Cγ and has been involved in mitogen-activated protein kinase signaling (Morandell *et al.*, 2008). P-Tyr1173 has been linked to phosphatidylinositol-3 kinase/Akt signaling, which results in stabilization of factors such as c-Myc, and further triggers EGFR de-phosphorylation and silencing (Segrelles *et al.*, 2006; Morandell *et al.*, 2008). In AK23-treated animals, EGFR steady-state protein levels were reduced, suggesting receptor activation and internalization (Sorkin and Goh, 2009), consistent with a significant increase in EGFR phosphorylation on Tyr1173. Phosphorylation of Tyr845 and Tyr992 was not significantly increased at this time point.

In contrast to a previous report (Berkowitz *et al.*, 2006), phosphorylation of p38 was not enhanced in AK23/PF- or AK23-treated neonatal skin at 24 hours, but c-Myc steady-state levels were significantly increased (Figure 1b and c). In non-junctional (Triton X-100 soluble) lysates, Dsg3 together with PG was increased in AK23/PF-treated animals and Dsg3 in AK23-treated animals (Figure 1d and e). In contrast, Dsg3 was markedly depleted from desmosomal (Triton X-100 insoluble) extracts in all AK23-treated mice, whereas other components such as desmocollin3 (Dsc3), Dsg1/2, and desmoplakin remained unchanged.

Consistent with findings in PV patients and PV IgG-injected neonatal mice (Williamson *et al.*, 2006, 2007a, b; Shu *et al.*, 2007; Pretel *et al.*, 2009), AK23 induced hyperproliferation in neonatal mice, which correlated with EGFR activation and c-Myc overexpression, as well as depletion of Dsg3 from desmosomes. Interestingly, AK23-induced molecular changes were largely similar with or without additional PF IgG, identifying injections with AK23 alone as a suitable test system to address the feasibility of adult mice for prospective studies on Dsg3 antibody-mediated signaling.

AK23-injected 8-week-old mice predominantly develop lesions in telogen HFs and oral mucosa
AK23-induced changes were then addressed in adult 8-week-old C57Bl/6J mice. After 24 hours, widespread PV-like blisters were observed in all AK23-treated animals in areas of mechanical stress, such as the hard palate, the esophagus, and the lip/snout skin (Figure 2a and b). Blisters were further present in the stem cell niche of the telogen HF known as the bulge, between the inner layer and the outer root sheath (Figure 2c) as reported for *Dsg3*-null mice (Koch *et al.*, 1998). At 24 hours, 75% of the follicles were affected, rising to 80% after 48 hours (Figure 2d). Macroscopically, this correlated with loosely anchored hair revealed by tape stripping (Figure 2e). In contrast, spontaneous clinical blisters rarely formed on back skin, in spite of evenly bound AK23 antibody in the basal cell layer (Figure 2a and b). However, widening of intercellular spaces, the earliest sign of loosening of intercellular contacts, was occasionally observed. Indicative of reduced food intake due to blisters in the oral cavity,
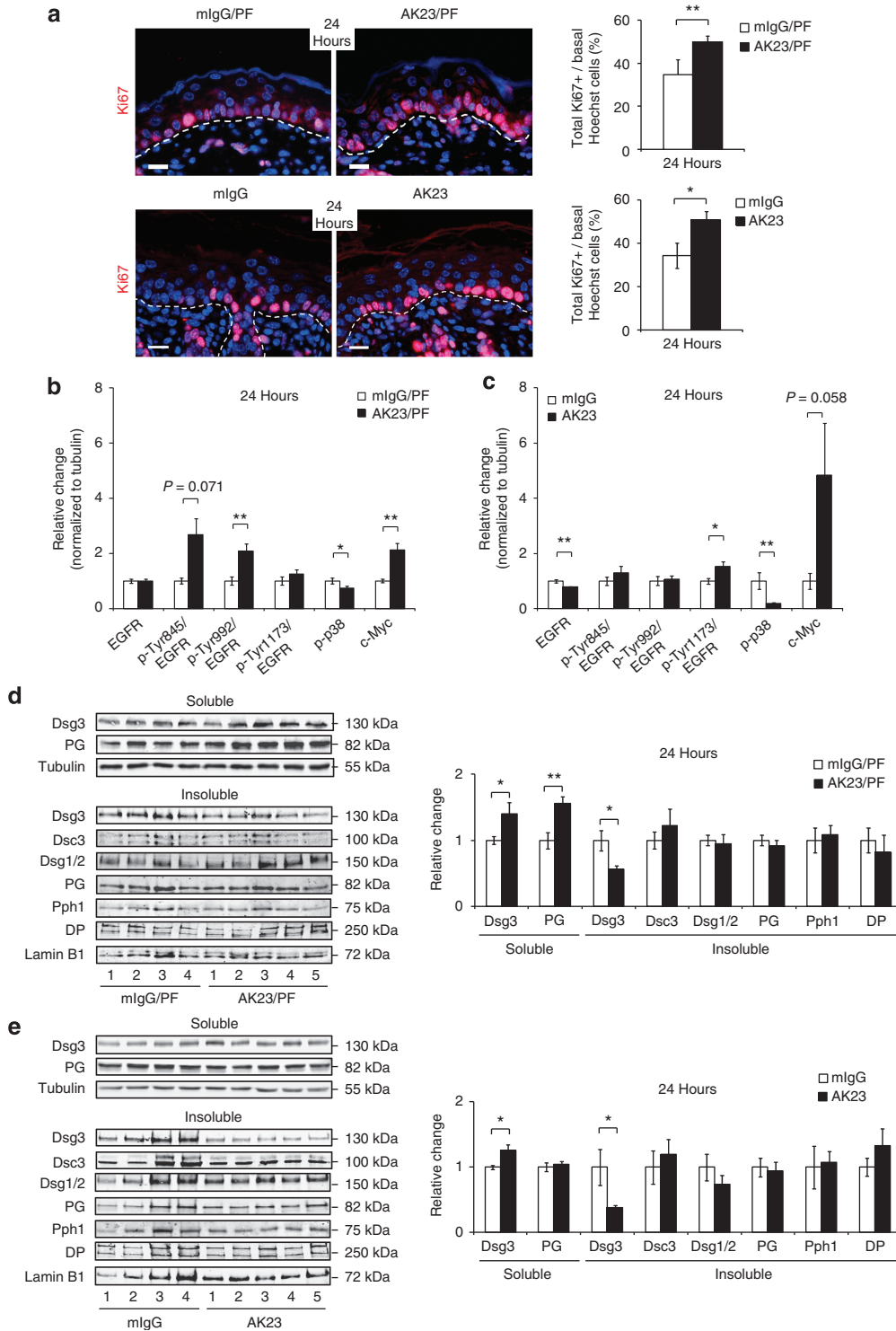
Figure 1. **AK23/PF IgG- and AK23-treated neonatal mice show hyperproliferation, EGFR activation, c-Myc upregulation, and depletion of Dsg3 from desmosomes.** (**a**) Shown are micrographs of immunofluorescence microscopy for Ki67 and graph of total Ki67+ cells in basal keratinocytes counted on micrographs of biopsies from neonatal mice injected with AK23 or control mIgG, with or without a half-maximal dose of PF IgG as indicated. More than 1,000 cells per animal were counted. Bar = 25 μm. (**b**, **c**) Graphs depict average quantitative results of immunoblots from indicated proteins in Triton X-100-soluble fractions at 24 hours. Signals on each blot were quantified, normalized to tubulin, and plotted relative to mIgG set as 1. (**d**, **e**) Immunoblots and graphs of indicated proteins from Triton X-100-soluble and -insoluble fractions. Lanes indicate different animals. Blots were normalized to tubulin (soluble fractions, upper panel) or lamin B1 (insoluble fractions, lower panel; shown is lamin B1 of blots probed for (**d**) Dsg3/Dsc3/PG/Pph1, (**e**) Dsg3/Dsg1/2/PG). Data are mean ± SEM (n(mIgG/PF; mIgG) = 4 and n(AK23/PF; AK23) = 5 animals); *$P \leqslant 0.05$ and **$P \leqslant 0.01$. AK23, mouse monoclonal pathogenic anti-Dsg3 antibody; DP, desmoplakin; Dsc, desmocollin; Dsg, desmoglein; mIgG, mouse IgG; PF, pemphigus foliaceus; PG, plakoglobin; Pph1, plakophilin.
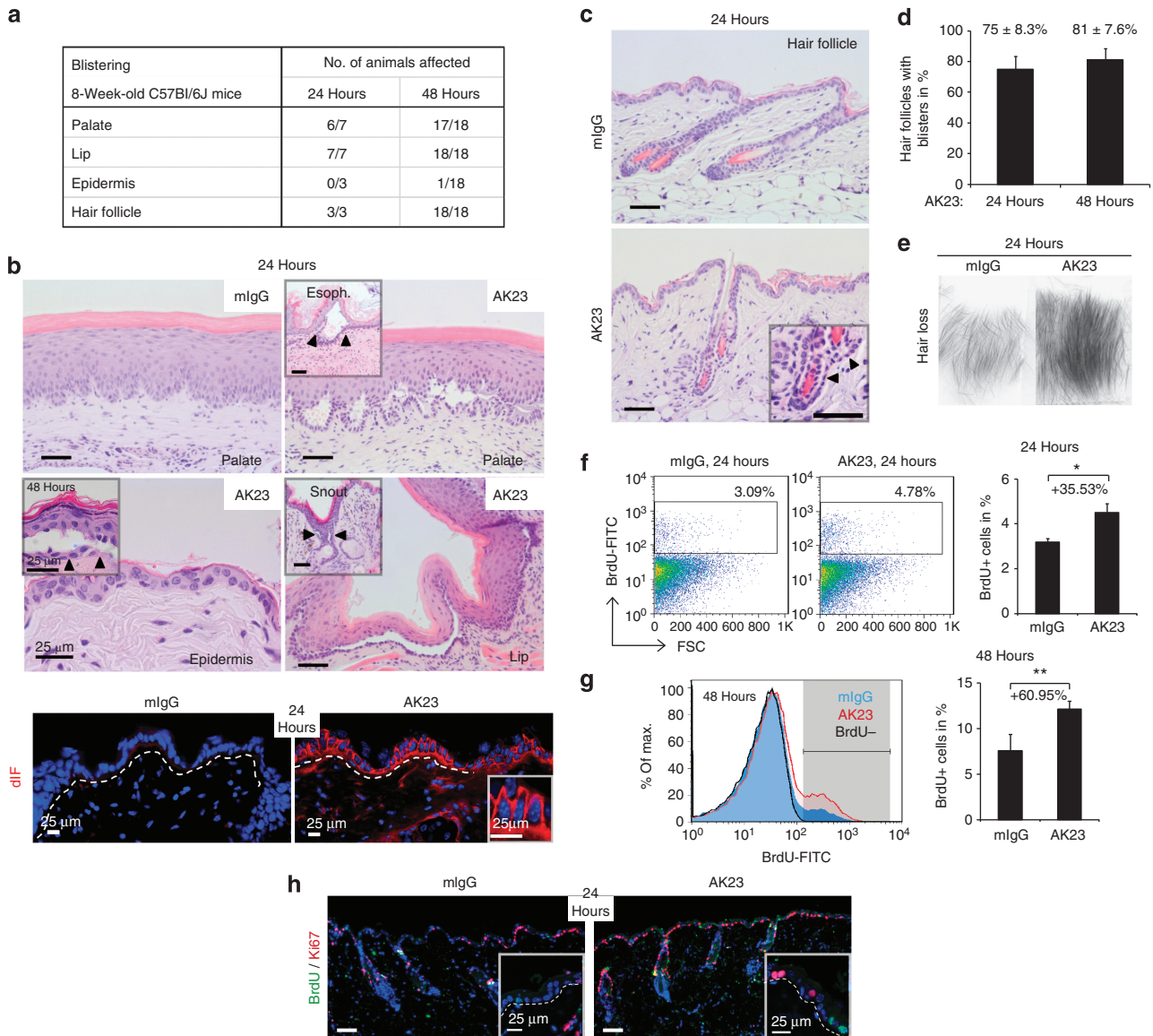
Figure 2. AK23-treated 8-week-old C57Bl/6J mice exhibit typical PV lesions and epidermal hyperproliferation. (**a**) Blister sites and number of affected/tested animals are summarized. (**b**) H&E-stained paraffin sections of indicated tissues show lesions, and direct immunofluorescence (dIF) microscopy depicts AK23 binding to basal epidermal keratinocytes. Inserts show lesions (arrowheads) in esophagus and snout skin and a rare lesion in the epidermis. (**c**) Histology and (**d**) percentage of HF blisters (insert, arrowhead) in AK23-treated animals. Data are mean ± SDM. HF analyzed (n(24 hours) = 115; n(48 hours) = 455). (**e**) Hair loss by tape stripping. (**f**) Representative flow cytometry blots for FSC and BrdU-labeled viable cells gated for BrdU-positive cells, and graph of average results. Data are mean ± SDM. ($n = 2$ animals per group; two experiments), *$P \leqslant 0.05$. (**g**) Representative flow cytometry histogram for BrdU-labeled cells and graph of average results. Data are mean ± SDM. ($n = 4$ animals per group). **$P \leqslant 0.01$. (**h**) Immunofluorescence microscopy depicting the distribution of BrdU-positive and Ki67-positive cells in epidermis (inserts: close up of epidermis). Bars = 50 μm or as indicated. AK23, mouse monoclonal pathogenic anti-Dsg3 antibody; Esoph., esophagus; FSC, forward scatter; H&E, hematoxylin and eosin; HF, hair follicle; max., maximum; mIgG, mouse IgG; PV, pemphigus vulgaris.

AK23-treated mice exhibited weight loss and were killed at 48 hours.

Eight-week-old Rag2−/− mice responded similarly to AK23 than C57Bl/6J mice, establishing that blister formation in response to AK23 does not involve a B- and T-cell-mediated immune response (Supplementary Figure S1 online).

AK23 induces hyperproliferation in 8-week-old mice
Proliferation in the epidermis of 8-week-old AK23- or mouse IgG (mIgG)-injected C57Bl/6J mice was assessed

by BrdU incorporation and Ki67 staining. Using flow cytometry, 35% more BrdU-positive cells were measured in AK23-treated mice as compared with control animals 24 hours after a single BrdU injection (Figure 2f), and 60% more BrdU-positive cells were measured at 48 hours after four consecutive BrdU injections (Figure 2g). Immunofluorescence microscopy visually confirmed increased BrdU incorporation and more numerous Ki67-positive cells in the basal layer of the epidermis and in HFs (Figure 2h).

Taken together, these results recapitulate the hyperproliferation in neonatal mice (shown here) and PV patients' epidermis (Williamson *et al.*, 2006).

AK23-treated 8-week-old mice exhibit EGFR activation, Myc upregulation, and increased non-junctional Dsg3

We then addressed the status of EGFR, p38, and Myc in Triton X-100-soluble protein fractions from back skin of 8-week-old C57Bl/6J mice, together with Dsg3, E-cadherin, and PG protein levels. Compatible with receptor activation (Sorkin and Goh, 2009), EGFR steady-state levels were already reduced 2 hours after AK23 injection, and the relative levels of mitotically active p-Tyr845 EGFR were on average increased by 2-fold (Figure 3a). Furthermore, phosphorylation of Tyr992 was weakly detectable in two animals out of four (but not measurable; data not shown) and Tyr1173 was unchanged. At 48 hours, phosphorylation of Tyr845 was no longer detectable, whereas that of Tyr1173 had increased in 2/2 C57Bl/6J mice and 4/4 mice of a different genetic background (Figure 3a, Supplementary Figure S2 online). EGFR phosphorylation correlated at 2 hours with an increase in cyclin D1, expressed in actively dividing cells, and at 48 hours with increased c-Myc and N-Myc but not L-Myc (Figure 3b). The latter changes were not yet seen at 24 hours (data not shown). At 48 hours, a tendency toward increased phosphorylation of p38 was observed. In the same lysates, 80% more non-junctional Dsg3 protein was measured at 2 hours in AK23-treated animals, which then returned to base levels (Figure 3c). No changes were observed for E-cadherin and PG.

On the mRNA steady-state level, *c-Myc* was significantly decreased at 2 hours in AK23-treated mice, whereas *N-Myc* and *cyclin D1* were increased (Figure 3d). *N-Myc* then continued to increase up to 24 hours, together with increased expression of *L-Myc* and *cyclin D2*. Except for *N-* and *L-Myc*, mRNA expression levels were back to normal at 48 hours.

In summary, between adult and neonatal AK23-injected mice, the molecular changes were largely similar, including
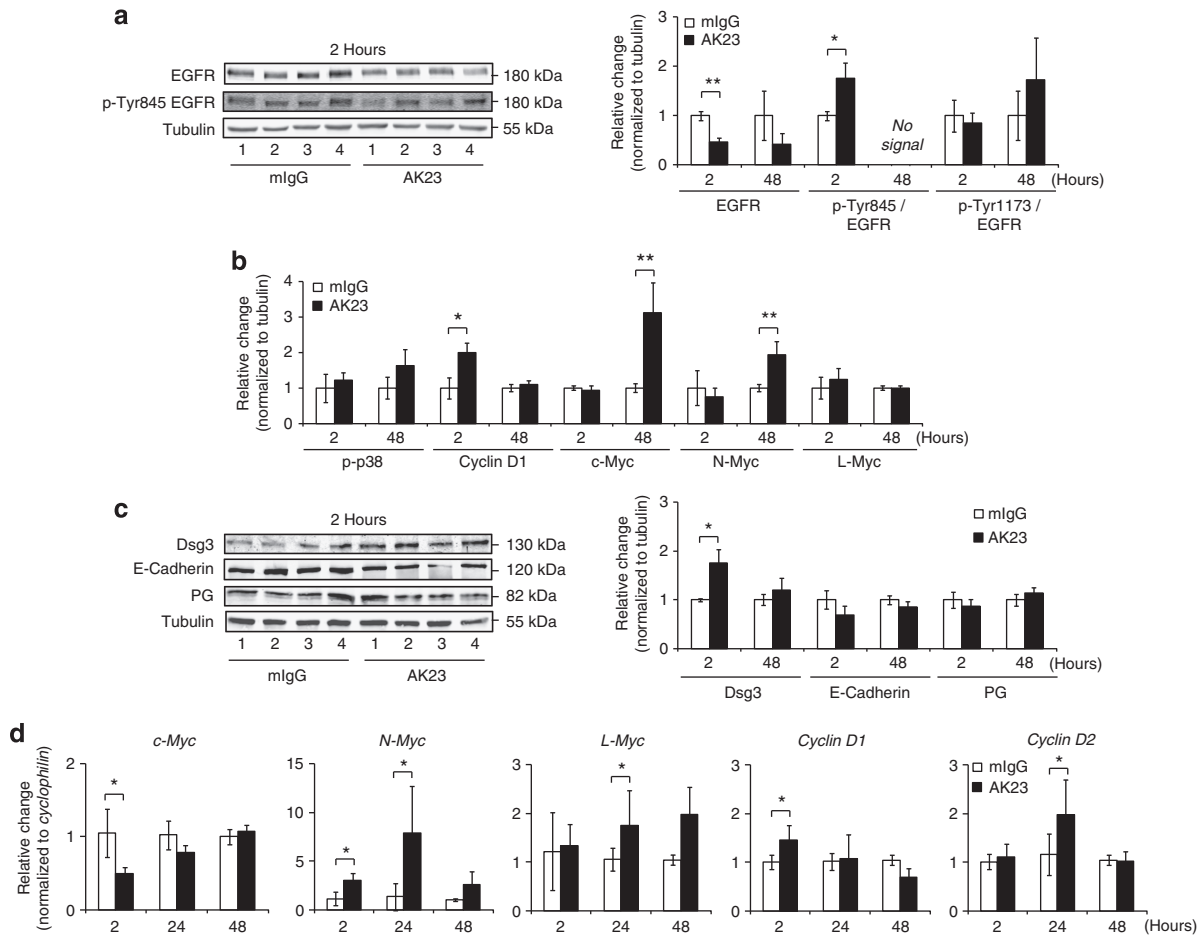

Figure 3. **EGFR is activated and Myc, cyclin D, and Dsg3 protein steady-state levels are significantly increased in Triton X-100-soluble fractions of AK23-treated 8-week-old C57Bl/6J mice.** (**a**) Immunoblots and graphs of average quantitative results are shown for indicated proteins at 24 and 48 hours. Signals were quantified, normalized to tubulin on each blot, and plotted relative to mIgG set as 1 (*n*(2 hours) = 4 animals per group; *n*(48 hours, mIgG) = 4, *n*(48 hours, AK23) = 2). (**b**) Graphs as in **a**, *n*(2 hours) = 4 animals per group, *n*(48 hours, mIgG) = 8 animals, *n*(48 hours, AK23) = 6 animals. (**c**) Similar to **a**, *n*(2 hours) = 4 animals per group, *n*(48 hours, mIgG) = 8 animals, *n*(48 hours, AK23) = 6 animals. (**a–c**) Data are mean ± SEM. **$P \leqslant 0.01$ and *$P \leqslant 0.05$. (**d**) Graphs show indicated mRNA steady-state levels obtained by quantitative RT-PCR. Values were normalized to *cyclophilin* and are plotted relative to mIgG set as 1 (*n*(2/24 hours) = 4 animals per group, *n*(48 hours, mIgG) = 8, *n*(48 hours, AK23) = 7 animals). Data are mean ± SEM. AK23, mouse monoclonal pathogenic anti-Dsg3 antibody; Dsg3, desmoglein 3; mIgG, mouse IgG; PG, plakoglobin; RT-PCR, reverse transcriptase PCR.

an increase in soluble Dsg3, potentially stemming from desmosome remodeling (Aoyama *et al.*, 2010). Furthermore, in adult mice, changes in mRNA preceded or coincided with changes in corresponding proteins, indicating *de novo* synthesis. The decrease in *c-Myc* mRNA might suggest a negative feedback loop involving an enhanced turnover rate following early transcriptional activation (Dai and Lu, 2008).

Dsg3 depletion from desmosomes is characteristic for AK23-treated 8-week-old mice

Desmosomal proteins were quantified in Triton X-100-insoluble fractions of 8-week-old C57Bl/6J mouse skin. Steady-state levels of junctional Dsg3 started to decrease at 24 hours, and were reduced to roughly 30% at 48 hours in all AK23-injected animals, whereas Dsc3 levels were largely unchanged (Figure 4). Dsg1/2 was not affected at 24 hours but significantly reduced at 48 hours, concomitant with a tendency toward a decrease in plaque proteins plakophilin and desmoplakin but not PG. On average, no significant differences in keratin expression were measured between treated and untreated animals. However, three out of four AK23-injected animals exhibited decreased keratin

15 expression, whereas keratin 14 levels were above that of the control in two out of four AK23-treated animals at 48 hours, both features of hyperproliferative epidermis (Werner and Munz, 2000).

Comparative immunofluorescence analyses performed on skin biopsies 24 and 48 hours after AK23 injection revealed no major changes in the expression pattern of epidermal markers, except for a reduction in Dsg1/2 and keratin 15 (Supplementary Figure S3 online, shows 48 hours). Decreased Dsg1/2 is a consistent feature of PV patients and PV antibody-challenged human organotypic and mouse keratinocyte cultures (Williamson *et al.*, 2006; van der Wier *et al.*, 2010).

AK23 induces a rapid interdesmosomal membrane detachment

To further correlate the AK23-induced signal activation to changes in desmosomal ultrastructure in 8-week-old C57Bl/6J mice, we performed electron microscopy. Two hours after AK23 injection, antibodies were already bound to the surface of basal keratinocytes, no blisters were observed by routine histology in the epidermis and HF, and only a small blister was present in the hard palate in one out of eight
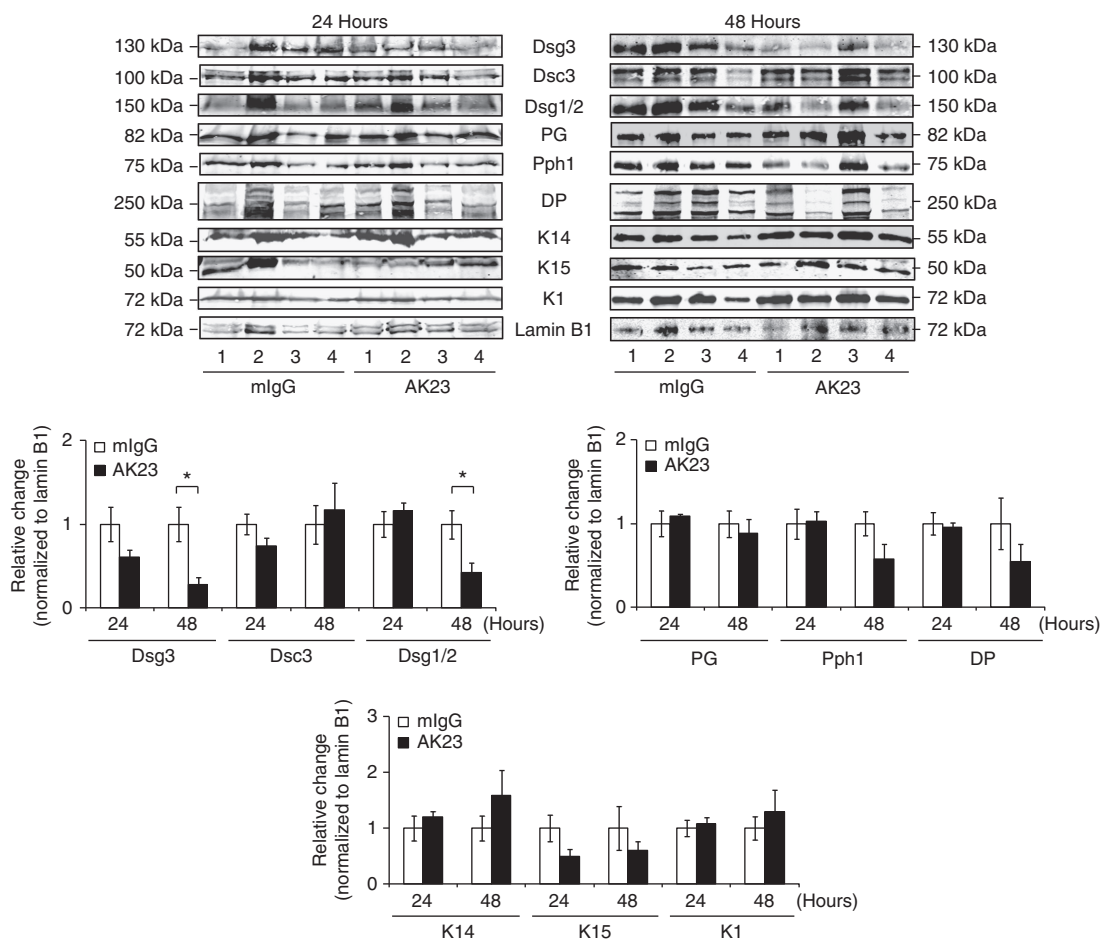

Figure 4. **Dsg3 is depleted from desmosomes in AK23-treated 8-week-old C57Bl/6J mice.** Immunoblot of the Triton X-100-insoluble fractions are shown for indicated proteins. Numbered lanes correspond to four different animals per group. Each blot was normalized with respect to lamin B1 (shown is the blot probed for Dsg3/K15 at 24 hours and for PG, K15/Pph1 at 48 hours). Signals were quantified, normalized, and are plotted relative to mIgG set as 1. Data are mean ± SEM (n(24 hours) = 4 animals per group; n(48 hours) = 4 animals per group), *$P \leqslant 0.05$. AK23, mouse monoclonal pathogenic anti-Dsg3 antibody; DP, desmoplakin; Dsc, desmocollin; Dsg, desmoglein; K(1,14,15), keratin (1,14,15); mIgG, mouse IgG; PG, plakoglobin; Pph1, plakophilin.

AK23-treated animals (Figure 5a). In spite of an intact epidermis, electron microscopy of the same animals showed basal keratinocytes that were still joined by desmosomes, but most exhibited widening of interdesmosomal spaces (Figure 5b). By 48 hours, microscopic tissue damage largely confined to basal cells indicated skin fragility.

Figure 5. **AK23 causes widening of the intercellular spaces after 2 hours and microblisters after 48 hours in basal keratinocytes of AK23-treated 8-week-old C57Bl/6J mice.** (**a**) Histology (upper panel) and direct immunofluorescence (dIF) analyses (lower panel) at 2 hours in samples processed for electron microscopy. Only one animal out of eight showed a microblister in the hard palate (insert) but not in the epidermis. Arrows indicate AK23 binding. Bar = 25 μm. (**b**) Electron microscopical pictures at 2 and 48 hours. Tissue damage is seen in basal cells but not in suprabasal cells or controls (*n*(2/48 hours) = 2 animals per group). Scale bars: as indicated. AK23, mouse monoclonal pathogenic anti-Dsg3 antibody; Dsg, desmoglein; mIgG, mouse IgG; SC, stratum corneum; *, widened intercellular spaces.

DISCUSSION

This study describes an adult passive transfer model of 8-week-old C57Bl/6J mice injected with the monospecific pathogenic Dsg3 antibody AK23 (Tsunoda *et al.*, 2003). We demonstrate that this mouse model reproduces molecular events observed in AK23-injected neonatal mice, as well as major features reported in PV.

Histopathologically, PV patients with Dsg3 antibodies (the mucosal dominant phenotype) develop oral blisters with rare clinical lesions in skin (Amagai *et al.*, 1999b) and occasional blisters in HFs. Hair loss is a characteristic clinical feature of PV patients, but telogen HF blisters may be overlooked because, unlike in mice, the telogen phase is short and human hair grows asynchronously (Koch *et al.*, 1998; Dr Michael Hertl). In line with other adult PV mouse models using adoptive transfer (Amagai *et al.*, 2000; Tsunoda *et al.*, 2003), passive transfer of AK23 into adult mice mimics these clinical features (Figure 2a).

Our observations are also consistent with previous *in vivo* and *in vitro* reports on Dsg3 depletion from desmosomes in PV (Aoyama and Kitajima, 1999; Calkins *et al.*, 2006; Williamson *et al.*, 2006; Shu *et al.*, 2007; Yamamoto *et al.*, 2007; Mao *et al.*, 2009), which are also seen in AK23-injected neonatal mice shown here. In the adult mouse model, a visible Dsg3 loss commenced at 24 hours without affecting other proteins. It was preceded by a transient increase in Triton X-100-soluble Dsg3, also observed in neonatal mice. This is compatible with the recent suggestion that PV IgG/Dsg3 immune complexes are rapidly excluded from desmosomes internalized and degraded without initially affecting other components such as desmoplakin (Aoyama *et al.*, 2010). Internalization and degradation of non-junctional Dsg3 is also in line with previous studies on cultured mouse and human keratinocytes (Aoyama and Kitajima, 1999; Calkins *et al.*, 2006; Williamson *et al.*, 2006; Yamamoto *et al.*, 2007). Our lysis conditions do not allow us to discriminate between surface-exposed and internalized non-junctional Dsg3. Internalization can therefore not be excluded and is indirectly supported by the early widening of interdesmosomal spaces, also described previously in PV IgG-injected neonatal mice (Takahashi *et al.*, 1985). This suggests that after AK23 injection, non-junctional Dsg3 molecules (and presumably other adhesion molecules) are no longer available for transadhesion outside of desmosomes. The increase in non-junctional Dsg3 returned to normal after 48 hours, indicative of degradation.
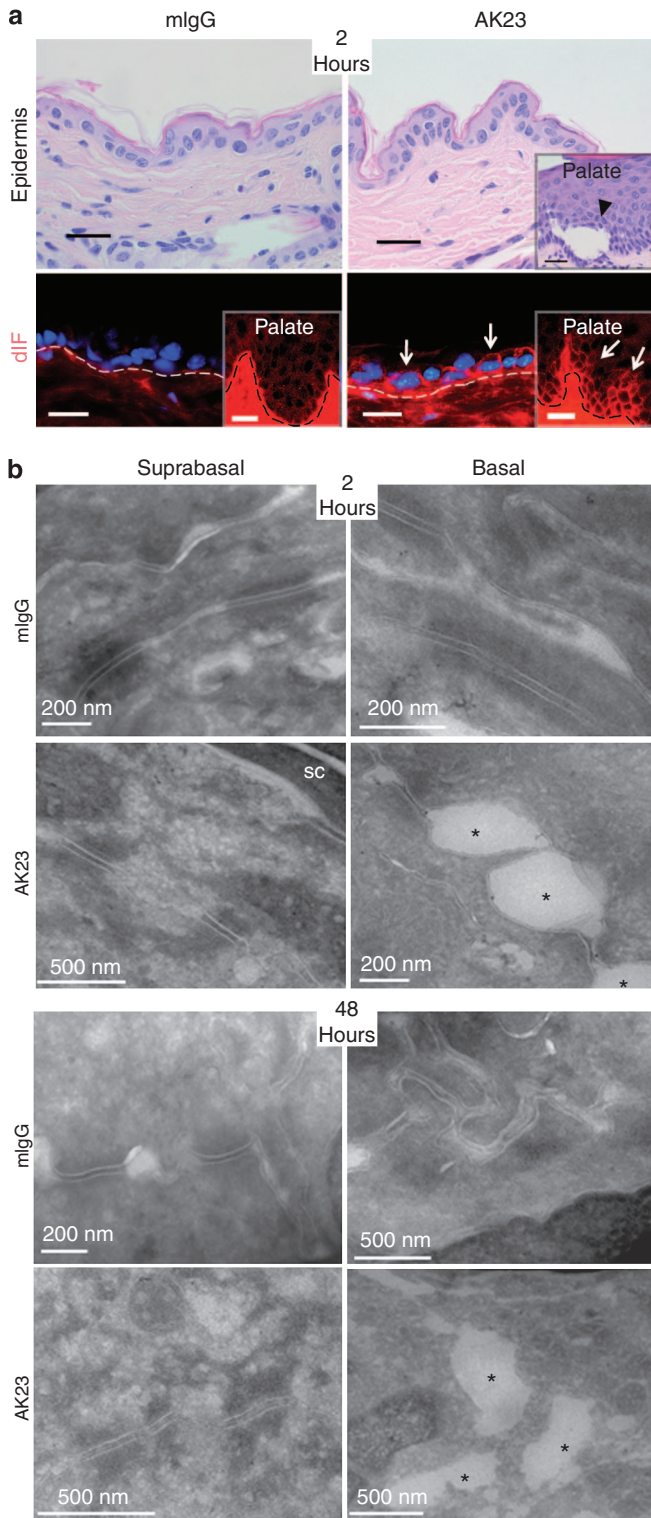
Consistent with numerous reports on PV IgG-treated keratinocytes, desmosome function was affected in the epidermis of adult mice at around 48 hours; the loss of additional desmosomal proteins such as Dsg1/2 and DP correlated with epidermal fragility in basal keratinocytes as underscored by microlesions and tissue damage. In line with the compensation hypothesis (Mahoney *et al.*, 1999), AK23-induced microlesions however rarely evolved into clinical blisters (Figure 2a), except in the presence of PF IgG, as seen in neonatal mice. In view of the similar activation of signaling molecules in AK23/PF- and AK23-treated mice at the time point analyzed, it appears that blister formation could be determined by either the length and strength of the signal or by complementary PF IgG-induced signaling. These possibilities can now be pursued further in comparison with the initial signals involved in desmosome remodeling in skin and adult HFs under defined pathological conditions. Together, these observations reveal that AK23 triggers a stepwise signal-driven mechanism that results in Nikolsky-positive skin with weakened desmosomes.

In addition to desmosomal proteins, we also investigated signaling molecules reported in PV to validate the adult mouse model for analyses on AK23-mediated signal induction. A recent study has suggested that p38 activation correlates with Dsc3 endocytosis and clinical blisters (Mao *et al.*, 2011). We did not observe a decrease in Dsc3 following AK23 treatment of adult or neonatal mice, and p38 showed only a tendency to be hyperphosphorylated at 48 hours. This may support the conclusion by the authors that p38 is not involved in mechanisms leading to Nikolsky-positive skin but contributes to clinical lesions. Alternatively, because PF IgG-injected neonatal mice showed a biphasic p38 activation scheme (Lee *et al.*, 2009), it can currently not be excluded that p38 activation occurred outside the time points investigated here.

Compatible with EGFR activation, we also observed increased proliferation, upregulation of cyclin as well as Myc isoforms in adult and neonatal mice. Although little is known about N-Myc and L-Myc in epidermis, balanced N-Myc expression was found to be essential for HF development and regeneration (Mill *et al.*, 2005). Furthermore, hyperproliferation and increased Myc/c-Myc have been associated with PV pathology and disease progression (Williamson *et al.*, 2006, 2007a). As previously shown, transcriptional activation of *c-Myc* resulted from PV IgG-mediated nuclear depletion of its repressor PG. Intriguingly, at 2 hours, we observed a decrease in *c-Myc* steady-state mRNA, whereas c-Myc protein was increased at 48 hours. This might indicate a negative feedback loop involving enhanced *c-Myc* turnover in response to transcriptional activation (Dai and Lu, 2008), followed by stabilization of c-Myc protein, for example, through EGFR-mediated phosphatidylinositol-3 kinase/Akt activation (Segrelles *et al.*, 2006). Indeed, hyperproliferation and Myc overexpression correlated with EGFR phosphorylation of Tyr845 (pro-mitogenic) and Tyr1173 (phosphatidylinositol-3 kinase/ Akt activation), respectively, which is consistent with EGFR activation reported in PV IgG-treated neonatal mice and various epidermoid cell types (Chernyavsky *et al.*, 2005; Frusic-Zlotkin *et al.*, 2006; Pretel *et al.*, 2009). Our current result on late phosphorylation of EGFR on Tyr1173 could further explain why this event was not observed in human keratinocytes 1 hour after treatment with PV IgG (Heupel *et al.*, 2009).

In summary, AK23 injection in this adult mouse model induced early molecular changes and widening of inter-cellular spaces in basal keratinocytes, followed by a stepwise series of changes in intracellular signaling and adhesion molecules reported in PV. Therefore, the adult passive transfer mouse model described here represents a valuable test system to further unravel the initial Dsg3 antibody-induced molecular changes in epidermis, HF, and stem cell niches of adult skin, and holds great promise as a test system for the validation of novel therapeutic indications in PV.

MATERIALS AND METHODS

Mice and passive transfer

Seven- to eight-week-old C57Bl/6J or B6. 129S6-Rag2[tm/Fwa]N12 (Taconic, Ry, Denmark) mice received a single subcutaneous injection of $12 \mu g\,g^{-1}$ body weight AK23 (a kind gift from Dr Masayuki Amagai, Tokyo; (Tsunoda *et al.*, 2003)) or normal mIgG (Equitech-Bio, Kerrville, TX) at the back as defined in a dose–response study ranging from $5 \mu g$ and $2.5 \,mg\,g^{-1}$ body weight AK23. Neonatal C57Bl/6J mice received $90 \mu g\,g^{-1}$ body weight AK23/mIgG with or without 1.5 mg PF IgG as described previously (Williamson *et al.*, 2006). Experiments were approved by the ethics committee, Canton Bern, Switzerland (26/08).

BrdU incorporation

Mice received 50 μg per g body weight BrdU (Sigma, Buchs, Switzerland; B5002) once intraperitoneally at the time point of AK23/mIgG injection and were killed at 24 hours, or alternatively received four times 50 μg per g body weight in 12-hour intervals before being killed at 48 hours.

Cell isolation and flow cytometry

Epidermis was incubated in Trypsin-EDTA/phosphate-buffered saline (PBS; 0.2%/0.08%; Amimed, Allschwil, Switzerland) for 2 hours at 32 °C, and keratinocytes were scraped off and dissociated in DMEM/10% fetal calf serum on a magnetic stirrer for 20 minutes. Cells were consecutively filtered through a 70-μm and 40-μm cell strainer (BD, Allschwil, Switzerland), washed with CnT-02 (CELLnTEC, Bern, Switzerland), and stained with the LIVE/DEAD Fixable Dead Cell Stain Kit BLUE (Invitrogen, Zug, Switzerland). The FITC BrdU Flow Kit was used (BD) following the manufacturer's protocol. Cells were gated for single cells and viability using a BD LSR II (BD), and 50,000 cells were analyzed using the FlowJo 7.5 (Tree Star, Ashland, OR).

Immunofluorescence microscopy

Routine histology, BrdU and Ki67 detections were done on paraffin-embedded biopsies. Heat-mediated antigen retrieval was performed for 3×5 minutes, using a microwave, in $0.01 \,M$ sodium citrate buffer, pH 6.0. Sections were blocked

with 5% NGS, 4% BSA in PBS$^+$ (containing 0.2 mM CaCl$_2$), incubated with BrdU (Clone BU1/75, Abcam, Luzern, Switzerland) or Ki67 (SP6, Rocklin, CA) antibodies in PBS$^+$ containing 2% BSA, 2.5% NGS, 0.2% Triton X-100 at 4 °C overnight, followed by treatment with anti-rabbit/rat IgG Alexa Fluor 488 or 594 (Invitrogen).

For direct immunofluorescence, frozen sections were prepared from OCT-embedded tissues (Tissue Tek, Sakura Torrance, CA). Sections of 8 μm were fixed for 10 minutes in 4% paraformaldehyde at room temperature, washed with PBS$^+$ followed by 20 mM glycine in PBS$^+$, and blocked in PBS$^+$ containing 2.5% NGS, 1% BSA, 2% gelatine, and 0.1% Triton X-100 for 1 hour at room temperature before incubation with anti-mIgG Alexa Fluor 488 for 1 hour at room temperature.

Protein extraction and western blot analyses

Mouse back skin was minced in lysis buffer (100 mM Tris HCl, pH 7.4, 150 mM NaCl, 1% Triton X-100, 10 mM NaF, 10 mM β-glycerophosphate, 10 mM Na$_3$VO$_4$, 1 mM PMSF, and complete protease inhibitor EDTA-free (Roche, Rotkreuz, Switzerland)) using a Polytron PT 1600E (Kinematica, Luzern, Switzerland). Lysates were incubated for 30 minutes on ice, and Triton X-100-soluble and -insoluble fractions were obtained after 10 minutes centrifugation at 12,000 r.p.m. and 4 °C. Insoluble fractions (pellet) were solubilized with 8 M urea, 1% SDS, 10% glycerol, 60 mM Tris, pH 6.8, 5% β-mercaptoethanol, and 1 mM phenylmethanesulfonylfluoride. Equal amounts of total protein were subjected to SDS-PAGE and transferred onto nitrocellulose or polyvinylidene difluoride (for EGFR) membranes. Signals were quantified using Odyssey (LICOR, Bad Homberg, Germany). Antibodies used are listed in Supplementary Methods online.

Quantitative reverse transcriptase PCR

Total RNA was extracted from mouse back skin using the RNeasy Fibrous Tissue kit (Qiagen, Hombrechtikon, Switzerland) according to the manufacturer's instructions and processed as described previously (Kolly *et al.*, 2005). Primers are described in Supplementary Methods online.

Electron microscopy

For cryopreservation, back skin samples were processed by a modified version of the Tokuyasu method (Peters *et al.*, 2006) as previously described (Scothern and Garrod, 2008).

Statistical analyses

Statistical analyses were performed using NCSS (Kaysville, UT). Significant differences between two groups were defined using the Student's *t*-test with $P \leqslant 0.05$.

SUPPLEMENTARY MATERIAL

Supplementary material is linked to the online version of the paper at http://www.nature.com/jid

REFERENCES

Amagai M, Komai A, Hashimoto T *et al.* (1999a) Usefulness of enzyme-linked immunosorbent assay using recombinant desmogleins 1 and 3 for serodiagnosis of pemphigus. *Br J Dermatol* 140:351–7

Amagai M, Tsunoda K, Suzuki H *et al.* (2000) Use of autoantigen-knockout mice in developing an active autoimmune disease model for pemphigus. *J Clin Invest* 105:625–31

Amagai M, Tsunoda K, Zillikens D *et al.* (1999b) The clinical phenotype of pemphigus is defined by the anti-desmoglein autoantibody profile. *J Am Acad Dermatol* 40:167–70

Anhalt GJ, Labib RS, Voorhees JJ *et al.* (1982) Induction of pemphigus in neonatal mice by passive transfer of IgG from patients with the disease. *N Engl J Med* 306:1189–96

Aoyama Y, Kitajima Y (1999) Pemphigus vulgaris-IgG causes a rapid depletion of desmoglein 3 (Dsg3) from the Triton X-100 soluble pools, leading to the formation of Dsg3- depleted desmosomes in a human squamous carcinoma cell line, DJM-1 cells. *J Invest Dermatol* 112:67–71

Aoyama Y, Nagai M, Kitajima Y (2010) Binding of pemphigus vulgaris IgG to antigens in desmosome core domains excludes immune complexes rather than directly splitting desmosomes. *Br J Dermatol* 162:1049–55

Berkowitz P, Hu P, Warren S *et al.* (2006) p38MAPK inhibition prevents disease in pemphigus vulgaris mice. *PNAS* 103:12855–60

Caldelari R, de Bruin A, Baumann D *et al.* (2001) A central role for the armadillo protein plakoglobin in the autoimmune disease pemphigus vulgaris. *J Cell Biol* 153:823–34

Calkins CC, Setzer SV, Jennings JM *et al.* (2006) Desmoglein endocytosis and desmosome disassembly are coordinated responses to pemphigus autoantibodies. *J Biol Chem* 281:7623–34

Chernyavsky AI, Arredondo J, Karlsson E *et al.* (2005) The Ras/Raf-1/MEK1/ERK signaling pathway coupled to integrin expression mediates cholinergic regulation of keratinocyte directional migration. *J Biol Chem* 280:39220–8

Chernyavsky AI, Arredondo J, Kitajima Y *et al.* (2007) Desmoglein versus non-desmoglein signaling in pemphigus acantholysis: characterization of novel signaling pathways downstream of pemphigus vulgaris antigens. *J Biol Chem* 282:13804–12

Dai MS, Lu H (2008) Crosstalk between c-Myc and ribosome in ribosomal biogenesis and cancer. *J Cell Biochem* 105:670–7

de Bruin A, Caldelari R, Williamson L *et al.* (2007) Plakoglobin-dependent disruption of the desmosomal plaque in pemphigus vulgaris. *Exp Dermatol* 16:468–75

Esaki C, Seishima M, Yamada T *et al.* (1995) Pharmacologic evidence for involvement of phospholipase C in pemphigus IgG-induced inositol 1,4,5-triphosphate generation, intracellular calcium increase, and plasminogen activator secretion in DJM-1 cells, a squamous cell carcinoma line. *J Invest Dermatol* 105:329–33

Frusic-Zlotkin M, Raichenberg D, Wang X *et al.* (2006) Apoptotic mechanism in pemphigus autoimmunoglobulins-induced acantholysis-possible involvement of the EGF receptor. *Autoimmunity* 39:563–75

Garrod DR, Merritt AJ, Nie Z (2002) Desmosomal cadherins. *Curr Opin Cell Biol* 14:537–45

Getsios S, Waschke J, Borradori L *et al.* (2010) From cell signaling to novel therapeutic concepts: international pemphigus meeting on advances in pemphigus research and therapy. *J Invest Dermatol* 130:1764–8

Hanakawa Y, Li H, Lin C *et al.* (2004) Desmogleins 1 and 3 in the companion layer anchor mouse anagen hair to the follicle. *J Invest Dermatol* 123:817–22

Heupel WM, Engerer P, Schmidt E *et al.* (2009) Pemphigus vulgaris IgG cause loss of desmoglein-mediated adhesion and keratinocyte dissociation independent of epidermal growth factor receptor. *Am J Pathol* 174:475–85

Ishii K, Amagai M, Hall RP *et al.* (1997) Characterization of autoantibodies in pemphigus using antigen-specific enzyme-linked immunosorbent assays with baculovirus-expressed recombinant desmogleins. *J Immunol* 159:2010–7

Ishizawar R, Parsons SJ (2004) c-Src and cooperating partners in human cancer. *Cancer Cell* 6:209–14

Koch PJ, Mahoney MG, Cotsarelis G *et al.* (1998) Desmoglein 3 anchors telogen hair in the follicle. *J Cell Sci* 111:2529–37

Kolly C, Suter MM, Muller EJ (2005) Proliferation, cell cycle exit, and onset of terminal differentiation in cultured keratinocytes: pre-programmed pathways in control of C-Myc and Notch1 prevail over extracellular calcium signals. *J Invest Dermatol* 124:1014–25

Lee HE, Berkowitz P, Jolly PS *et al.* (2009) Biphasic activation of p38MAPK suggests that apoptosis is a downstream event in pemphigus acantholysis. *J Biol Chem* 284:12524–32

Mahoney MG, Wang Z, Rothenberger K *et al.* (1999) Explanations for the clinical and microscopic localization of lesions in pemphigus foliaceus and vulgaris. *J Clin Invest* 103:461–8

Mao X, Choi EJ, Payne AS (2009) Disruption of desmosome assembly by monovalent human pemphigus vulgaris monoclonal antibodies. *J Invest Dermatol* 129:908–18

Mao X, Sano Y, Park JM *et al.* (2011) p38 MAPK activation is downstream of the loss of intercellular adhesion in pemphigus vulgaris. *J Biol Chem* 286:1283–91

Mill P, Mo R, Hu MC *et al.* (2005) Shh controls epithelial proliferation via independent pathways that converge on N-Myc. *Dev Cell* 9:293–303

Morandell S, Stasyk T, Skvortsov S *et al.* (2008) Quantitative proteomics and phosphoproteomics reveal novel insights into complexity and dynamics of the EGFR signaling network. *Proteomics* 8:4383–401

Müller EJ, Williamson L, Kolly C *et al.* (2008) Outside-in signaling through integrins and cadherins: a central mechanism to control epidermal growth and differentiation? *J Invest Dermatol* 128:501–16

Osada K, Seishima M, Kitajima Y (1997) Pemphigus IgG activates and translocates protein kinase C from the cytosol to the particulate/cytoskeleton fractions in human keratinocytes. *J Invest Dermatol* 108:482–7

Peters PJ, Bos E, Griekspoor A (2006) Cryo-immunogold electron microscopy. *Curr Protoc Cell Biol* Chapter 4:Unit 4.7

Pretel M, Espana A, Marquina M *et al.* (2009) An imbalance in Akt/mTOR is involved in the apoptotic and acantholytic processes in a mouse model of pemphigus vulgaris. *Exp Dermatol* 18:771–80

Sanchez-Carpintero I, Espana A, Pelacho B *et al.* (2004) *In vivo* blockade of pemphigus vulgaris acantholysis by inhibition of intracellular signal transduction cascades. *Br J Dermatol* 151:565–70

Schneider MR, Schmidt-Ullrich R, Paus R (2009) The hair follicle as a dynamic miniorgan. *Curr Biol* 19:R132–42

Scothern A, Garrod D (2008) Visualization of desmosomes in the electron microscope. *Methods Cell Biol* 88:347–66

Segrelles C, Moral M, Lara MF *et al.* (2006) Molecular determinants of Akt-induced keratinocyte transformation. *Oncogene* 25:1174–85

Shu E, Yamamoto Y, Aoyama Y *et al.* (2007) Intraperitoneal injection of pemphigus vulgaris-IgG into mouse depletes epidermal keratinocytes of desmoglein 3 associated with generation of acantholysis. *Arch Dermatol Res* 299:165–7

Sorkin A, Goh LK (2009) Endocytosis and intracellular trafficking of ErbBs. *Exp Cell Res* 315:683–96

Stanley JR, Amagai M (2006) Pemphigus, bullous impetigo, and the staphylococcal scalded-skin syndrome. *N Engl J Med* 355:1800–10

Takahashi Y, Patel HP, Labib RS *et al.* (1985) Experimentally induced pemphigus vulgaris in neonatal BALB/c mice: a time-course study of clinical, immunologic, ultrastructural, and cytochemical changes. *J Invest Dermatol* 84:41–6

Tsunoda K, Ota T, Aoki M *et al.* (2003) Induction of pemphigus phenotype by a mouse monoclonal antibody against the amino-terminal adhesive interface of desmoglein 3. *J Immunol* 170:2170–8

van der Wier G, Pas HH, Jonkman MF (2010) Experimental human cell and tissue models of pemphigus. *Dermatol Res Pract* 2010:143871

Watt FM, Frye M, Benitah SA (2008) MYC in mammalian epidermis: how can an oncogene stimulate differentiation? *Nat Rev Cancer* 8:234–42

Werner S, Munz B (2000) Suppression of keratin 15 expression by transforming growth factor beta *in vitro* and by cutaneous injury *in vivo*. *Exp Cell Res* 254:80–90

Williamson L, Hunziker T, Suter MM *et al.* (2007a) Nuclear c-Myc: a molecular marker for early stage pemphigus vulgaris. *J Invest Dermatol* 127:1549–55

Williamson L, Raess NA, Caldelari R *et al.* (2006) Pemphigus vulgaris identifies plakoglobin as key suppressor of c-Myc in the skin. *EMBO J* 25:3298–309

Williamson L, Suter MM, Olivry T *et al.* (2007b) Upregulation of c-Myc may contribute to the pathogenesis of canine pemphigus vulgaris. *Vet Dermatol* 18:12–7

Yamamoto Y, Aoyama Y, Shu E *et al.* (2007) Anti-desmoglein 3 (Dsg3) monoclonal antibodies deplete desmosomes of Dsg3 and differ in their Dsg3-depleting activities related to pathogenicity. *J Biol Chem* 282:17866–76